https://doi.org/10.5194/egusphere-2023-2330
Preprint. Discussion started: 30 November 2023

Kelp Forest model development in the *Coupled Ocean-Atmosphere-Wave-Sediment-Transport model (COAWST V3.4*)

Matheus Fagundes[1]; Fiorenza Micheli[2,3]; Stephen G. Monismith[4]; Arnoldo Valle-Levinson[5]; C. Brock Woodson[1]

[1] Department of Engineering, University of Georgia, Athens, GA, USA

[2]Ocean Department, Hopkins Marine Station, Stanford University, Pacific Grove, CA, USA

[3]Stanford Center for Ocean Solutions, Pacific Grove, CA, USA

[4]Monterey Bay Aquarium Research Institute, Moss Landing, CA, USA

[5]Civil and Coastal Engineering Department, University of Florida, Gainesville, FL, USA

Corresponding author:
Matheus Fagundes, mf99274@uga.edu

ABSTRACT

Kelp forests are essential ecosystems in coastal regions around the world. They have large effects on flow structure, biogeochemical processes, and ecological dynamics. However, studies have yet to simulate these ecosystems in either regional ocean or global climate models. Here we describe and validate a model that simulates kelp forests in the water column for the ocean component of the *Coupled Ocean-Atmosphere-Wave-Sediment-Transport model (COAWST V3.4*) using a simple yet efficient linear regression approach to simulate kelp canopies. An *in-situ* dataset of 2-1/2 years, with and without kelp forest coverage around Isla Natividad (Baja CA, MX), allowed model validation for the main tidal constituents. *We tested different* vegetation drag coefficients and compared simulations with our canopy model against the standard vegetation module in *COAWST*. Results show that while both models simulate the velocities observed in the *in situ* dataset reasonably well, our model better represents turbulence

https://doi.org/10.5194/egusphere-2023-2330
Preprint. Discussion started: 30 November 2023

kinetic energy through the water column as observed in laboratory experiments. This new kelp model can be helpful in ecology, physics, and biogeochemistry studies.

https://doi.org/10.5194/egusphere-2023-2330
Preprint. Discussion started: 30 November 2023

1 INTRODUCTION

Kelp forest ecosystems occupy almost 7 x 10^6 km^2 globally, when accounting for polar regions of the world's coastlines (Duarte, 2017; Macreadie *et al.*, 2019; Wernberg *et al.*, 2019), representing the largest coastal vegetated ecosystem in the world. Kelp lives in nutrient-rich habitats such as Eastern Boundary currents (EBUs) and provides significant global carbon sequestration either through respiration or carbon burial (Mcleod *et al.*, 2011; Britton *et al.*, 2016; Low *et al.*, 2021, Eger *et al.*, 2023). While kelp forests are important for global carbon sequestration (Macreadie *et al.*, 2019), kelp forests also have local biological (Gaylord *et al.*, 2002; Steneck *et al.*, 2003*)* and physical impacts (Gaylord *et al.*, 2007) that have been observed *in situ* (Walter *et al.*, 2012; Leary *et al.*, 2017; Monismith *et al.*, 2022) and in laboratory experiments (Rosman *et al.*, 2010; Rosman *et al.*, 2013). Considering that kelp forests have ecological, biogeochemical, and physical importance, comparative efforts to simulate these ecosystems in ocean models have been limited. Up to now, only one study has attempted to include the physical response of flows due to kelp forests into an ocean model, and it did not specifically account for variation in kelp canopy (Wu *et al.*,2017).

Kelp forests are found worldwide (Delille *et al.*, 2009; Schiel and Foster, 201t; Krause-Jensen *et al.*, 2016) and composed of 5 recognized types based on dominant genus: Ecklonia, Nereocystis, Lessonia, Laminaria, and Macrocystis (Rafaelli & Hawkins, 1999). Along the west coast of North America, the predominant species is the giant kelp *Macrocystis* spp. (Steneck *et al.*, 2002). *Macrocystis* spp. are found generally between 2 to 30 meters in the water column (Jackson & Winant, 1983) forming dense underwater forests (Steneck *et al.*, 2002) (Fig. 3.1). Kelp forests are recognized for their importance as shelter for macroinvertebrates, fish, and mammals (Dayton, 1985; Rafaelli & Hawkins, 1999). Furthermore, kelp forests greatly impact carbon storage or net

https://doi.org/10.5194/egusphere-2023-2330
Preprint. Discussion started: 30 November 2023

primary productivity (NPP). A kelp forest can uptake up to 4-fold more carbon per year than a boreal forest (Reed & Brzezinski, 2009) or phytoplankton production in upwelling zones (Behrenfeld & Falkowski, 1997). Kelp forests account for almost 5% of the total global blue carbon and 1/3 of the total carbon sequestered in coastal regions (Filbee-Dexter & Wernberg, 2020; Eger *et al.*, 2023). Similarly, kelp forests alter currents and mixing in subtidal nearshore environments of temperate and high latitudes (Dayton, 1985; Rafaelli & Hawkins, 1999) and can dampen headland upwelling processes (Valle-Levinson *et al.*, 2022).

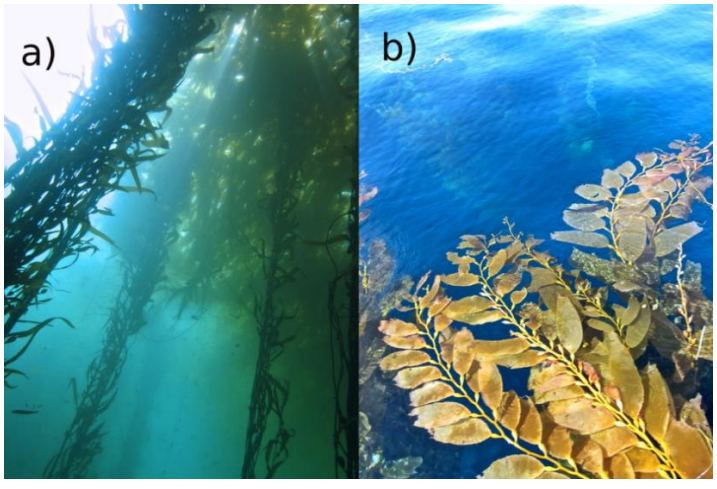

Figure 1 - Underwater formation of *M. Pyrifera* (a) and surface canopies at the surface (b). Source: Photos taken by Charles Boch and modified by Matheus Fagundes.

Previous studies to understand the effect of kelp forests on currents focused on particular regions along the California Current System (CCS; e.g: Jackson, 1984; Monismith *et al.*, 2022), scaled laboratory experiments (e.g: Rosman *et al.*, 2010), or high-resolution simulation of kelp beds (e.g: Wu *et al.*, 2017). While these studies helped better understand flow-vegetation interactions in these complex ecosystems, they did not capture the entire range of effects that kelp forests have on the

https://doi.org/10.5194/egusphere-2023-2330
Preprint. Discussion started: 30 November 2023

biology, biogeochemistry, and currents. In this present study, a high-resolution semi-idealized hydrodynamic model coupled with a vegetation module is used to create and validate a kelp module to allow for studies on the effects of kelp forests, not only on the hydrodynamics, but also the resultant effects on biogeochemical cycling and larval transport.

2 THEORY

The alongshore (v) momentum term of the Reynolds-Averaged Navier-Stokes (RANS) equations under the Boussinesq approximation (Beudin *et al.*, 2017) can be written as:

$$\frac{\partial v}{\partial t} + \frac{\partial vu}{\partial x} + \frac{\partial vv}{\partial y} + \frac{\partial vw}{\partial z} + fu = -\frac{1}{\rho_0}\frac{\partial P}{\partial y} - \frac{\partial}{\partial z}(\bar{u'w'} - \nu\frac{\partial v}{\partial z}) + D_v + F_v \qquad \textbf{(1)}$$

where $\frac{dv}{dt}$ is the unsteady term, $\frac{d(uv)}{dx} + \frac{d(vv)}{dy} + \frac{d(vw)}{dz}$ are the advection terms, f is the Coriolis parameter, $-\frac{1}{\rho_0}\frac{dP}{dy}$ is the pressure gradient in the y-direction, ρ_0 is the reference density of seawater, $\overline{u`w`}$ is the vertical flux of horizontal momentum by turbulent velocity fluctuations, v is the molecular viscosity, D_v is the horizontal diffusive term, and the last term (F_v) is a forcing term that includes the effects of vegetation on the flow. The spatially averaged vegetation drag force for the alongshore velocity neglecting cross shore velocity can be written as:

$$F_{d,veg,v} = \frac{1}{2}C_d pd P_d \sqrt{v^2} \qquad \textbf{(2)}$$

Where P_d is plant density (plants m^{-2}), pd is the width of kelp (m) or diameter in the case of kelp, and C_d is the drag coefficient for an individual plant. The code for the vegetation module in *COAWST* was originally written to represent seagrasses, which do not extend to the water surface, and therefore, no canopy was included. In these situations, the spacing between plants is constant to the surface (Fig. 2a). However, kelp forests can have extensive canopies that cover the last meter or so to the surface **(**Fig. 1; Traiger *et al.*, 2022). To date, the effects of surface canopies on currents

https://doi.org/10.5194/egusphere-2023-2330
Preprint. Discussion started: 30 November 2023

have only been studied in laboratory settings (Rosman *et al.*, 2013). However, kelp canopies can be represented using a linear regression to allow individual plants to get closer together and the kelp forest to become denser as the surface is approached (Fig. 2b). The second term important for the development of our approach is plant thickness (*pt*). The *pt* is inversely proportional to the *pd* in the second moment of area (*I*) equation (=$pdpt^3/12$) for the rectangle shape that was used by Beudin *et al.*, (2017). While not ideal, we decided to keep the same equation for *I*.

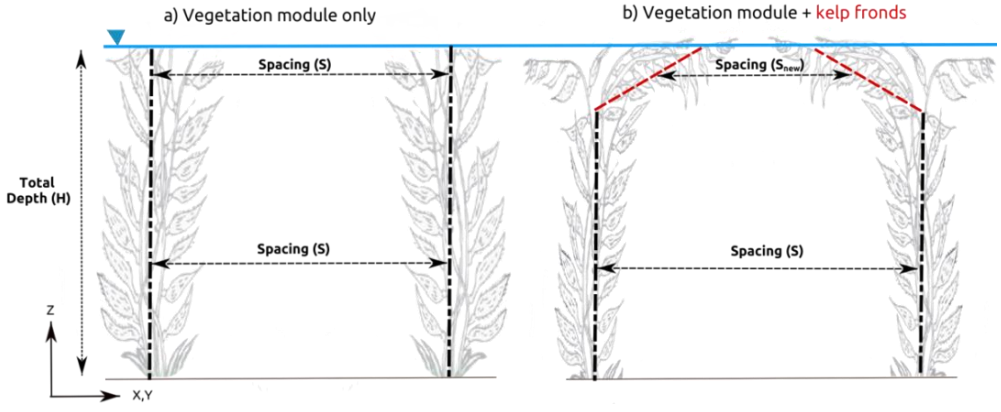

Figure 2 - Schematic of the two simulations in COAWST.

3 METHODS

3.1 Kelp canopy module

To account for kelp canopy, we developed a simple linear regression model that increases *pt* and *pd* near the surface as:

$$\begin{cases} pt = pd = 0.3 & if \;\; depth \leq 12m \\ pt = pd = 2.3 * depth - 27.3 & if \;\; depth \leq 12m \end{cases} \quad (3)$$

This modification in the vegetation model code captures the increase in kelp spacing (*S*) at the surface between individual kelp plants. For our scenario, this gives *pt* and *pd* equal to 2.3 at the surface, forming a virtually solid boundary. The coefficients in (3) can be varied to adjust for the

https://doi.org/10.5194/egusphere-2023-2330
Preprint. Discussion started: 30 November 2023

density, extent of the canopy, or water depth accordingly. The values reported are specific setup to our model test case.

Two simulations are presented in this paper: The first simulation is running the *COAWST* vegetation module with no changes (*standard* hereafter) (Fig. 2a), and the second is modifying the code to account for kelp canopy (*canopy*) (Fig. 2b). The *standard* simulation assumes that *pd* and *pt* are constant from the seafloor to the surface. The *canopy* simulation assumes a linear increase in *pd* and *pt* in the last meter of the water column **(**Fig. 3.2; Utter & Denny, 1996). The *canopy* module (eqn. 3) simulates the effects of kelp stipes and fronds getting close to each other (*S*) as they spread out on the surface as they are longer than the water depth (Fig. 2b). The stipes and fronds are then represented by changing *pd* and *pt* and, consequently, the effects of kelp forests on the currents. These differences in *pd* and *pt* directly affect the bulk drag in the water column, consequently changing the depth-averaged velocity and turbulence.

3.2 Area of Study

This study focuses on kelp forests surrounding Isla Natividad in the Vizcaino Bay region of Baja California, MX. Baja California is affected by large scale forcings such as El Niño (Trenberth, 1997) and marine heat waves (Cavanaugh *et al.*, 2010; McPherson *et al.*, 2021). Mesoscale forcings such as California Current characterized by low salinity, low temperature, high dissolved oxygen (DO) and California Undercurrent (CU) that is saltier, higher temperature and low in dissolved oxygen, also play a major role in the physical environment of this region (Mancilla-Peraza *et al.*, 1993). Seasonally, there is a marked stratification in the upper 20 meters of the water column, and conditions are influenced by wind-driven upwelling that brings water temperatures as low as 8°C, salinity (~33.8), and low DO (<5.5 ml/l) to the surface during spring/summer. During winter, waters can reach 16°C, salinity (~34), and DO around 5ml/l (Mancilla-Peraza *et*

https://doi.org/10.5194/egusphere-2023-2330
Preprint. Discussion started: 30 November 2023

al., 1993). Around Isla Natividad, winds, waves (surface and internal), tides, and kelp forests drive the dynamics (Woodson *et al.*, 20[illegible]Valle-Levinson *et al.*, 2022) at relatively small spatial and temporal scales (e.g: < 1 km, < 24 h). For instance, the shape of kelp forests can modify tides and dampen headland upwelling (Valle-Levinson *et al.*, 2022).

Isla Natividad is a 7 km long island south of Isla Cedros in Central Baja California, Mexico (Schlenger *et al.*, 2021) located between 115°15'W-115°6'W and 27°48'N-27°55'12''N (Fig. 3). The island is bounded by Kellet Channel on the north and Dewey Channel on the south (Mancilla-Peraza *et al.*, 1993), and is surrounded year-round by kelp forests (*Macrocystis Pyrifera*) which provide shelter for organisms including abalones (*Haliotis* spp.; Micheli *et al.*, 2012). Isla Natividad has two distinct local ocean regions on each side of the island (Woodson, 2018). On the southeastern side, Morro Prieto can reach mean temperature of 16°C and mean DO of 6 mg/l at 12 m while on the northwestern side, Punta Prieta has waters that are typically 3°C warmer and mean DO of 7.5 mg/l (Boch *et al.*, 2018) at the same depth. Because of the economic and ecological importance of abalone, the fishing cooperative, Buzos Y Pescadores, in Isla Natividad established 2 marine reserves that have been monitored since 2006 (Boch *et al.*, 2018; Micheli *et al.*, 2012). One of the marine reserves is located near Punta Prieta and has oceanographic sensors (CTDs, MiniDOTs, thermistors, and adps) at 7 m and 12 m depth (Boch *et al.*, 2018).

https://doi.org/10.5194/egusphere-2023-2330
Preprint. Discussion started: 30 November 2023

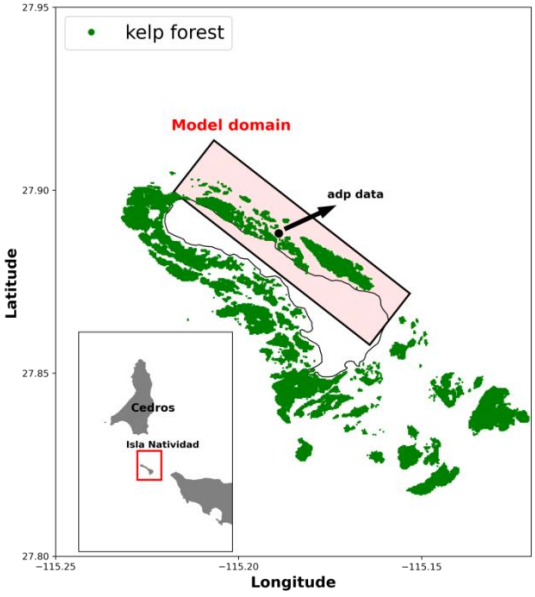

Figure 3 - Map of Isla Natividad indicating regional location and areas covered with kelp. Black circle indicates location of adp data used in this study. Punta Prieta, on the northeastern side of Isla Natividad.

3.3 Forcing

The mooring at Punta Prieta (Fig. 3) was chosen for evaluating the vegetation models in *COAWST* for four reasons, a) long-term data are available (Woodson, 2018), b) a heat wave in 2015-16 complete removal of kelp **(**Fig. 4**)** allowing understanding the environment without kelp (Monismith et al 2022), c) it is within a marine reserve thereby providing a relatively undisturbed habitat (Micheli *et al.*, 2012), and d) flows are generally tidal and alongshore in contrast to flows around Morro Prieto (Boch *et al.*, 2018).

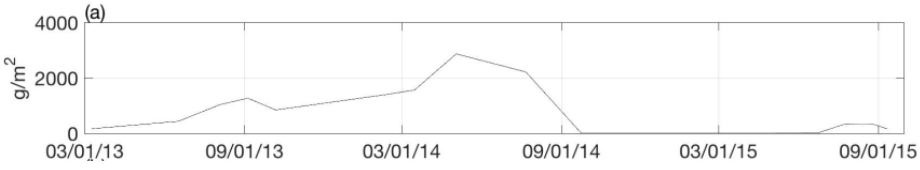

Figure 4 - Averaged kelp biomass around Isla Natividad, MX. Source: Monismith et al., 2022.

https://doi.org/10.5194/egusphere-2023-2330
Preprint. Discussion started: 30 November 2023

In situ current data were collected every 0.5 meter starting from 0.65 meters above the bottom to the surface (~14 m) from 2013-2016 using a 1MHz Nortek Aquadopp (*adp*; Fig. 3.5). The depth of the adp data used for this simulation was from 2.65-12.65 meters from the bottom to remove errors in the first couple of meters due to sidelobe interference (Lentz *et al.*, 2022). Depth-averaged velocities were calculated after removing errors from bottom and surface (Supplementary Fig. 1). Both E-W and N-S velocities increased in the 2015 period (Supplementary Fig. 1) when there was no kelp biomass observed (Fig. 4) while in 2014, the highest kelp biomass observed for the 2-1/2 year record, velocities were ~2-fold slower (Monismith *et al.*, 2022).

Currents were rotated into along- and cross-shore axes using Principal Component Analysis (PCA; Campbell & Atchley 1981; Emery & Thompson 2004). The rotated velocities were separated by season (Fig. 5). Based on Fig. 4 and Fig. 5, the cross-shore and alongshore Winter 2015 (henceforth *adp*15) and Spring 2014 (*adp*14) velocity records are used for no-kelp and kelp analyses. The adp15 data set was used to validate *COAWST* without the vegetation module before implementing it for the adp14 dataset (e.g., to estimate drag coefficients in the absence of kelp).

https://doi.org/10.5194/egusphere-2023-2330
Preprint. Discussion started: 30 November 2023

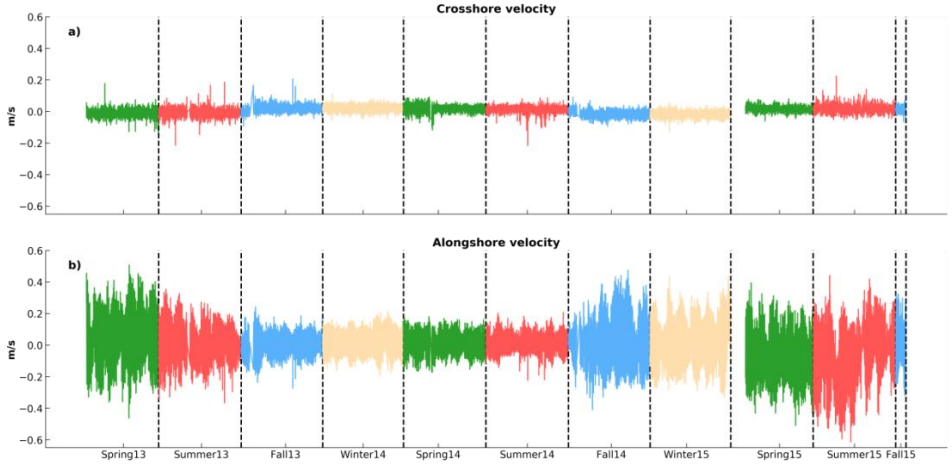

Figure 5 - Rotated cross-shore and alongshore velocities separated by season.

Both, cross-shore and alongshore velocities from adp15 and adp14 were harmonically analyzed using a python version of T-TIDE (Pawlociwicz *et al.*, 2002**;** Figs. 3.7, 3.8**)** before being used to force *COAWST* and to validate the vegetation module, respectively.

3.4 Numerical Model Description

The model used in this study was the *Coupled Ocean-Atmosphere-Wave-Sediment-Transport model (COAWST V3.4*; Warner *et al*., 2008). The ocean component of *COAWST* is the *Regional Ocean Modeling System (ROMS)* (Haidvogel *et al.*, 2008). ROMS is a 3-D, free-surface model that solves the primitive equations using hydrostatic and Boussinesq approximations with topography-following sigma layers (Shchepetkin and McWilliams, 2005; Haidvogel *et al.*, 2008). For the momentum equations, splines vertical advection and logarithmic bottom friction were selected to keep stability and better represent the environment, respectively. The model used the Mellor-Yamada level 2.5 turbulence closure scheme (MY-2.5). All boundaries (N,S,E,W) allowed along- and cross-shore flows. A periodic boundary condition was applied for free-surface, a Flather

https://doi.org/10.5194/egusphere-2023-2330
Preprint. Discussion started: 30 November 2023

condition for 2D u- and v-momentum, and a Radiation-Nudging condition for 3D u- and v-momentum.

The barotropic time-step was set at 10 s. Bottom roughness (z_{ob}) was 0.03 m and surface roughness (z_{os}) was 0.4 m with a no-slip condition along the bottom to provide a best fit for the no-kelp simulations to observed velocity profiles. The model had 40 sigma-layers splitting the 13 meters of water column with surface stretching (θ_s) = 1, bottom stretching (θ_b) = 2, and thermocline depth (Tcline) = 0. The domain was approximately 14 km long by 3 km wide **(**Fig. 6**)** with a grid size of 25 meters x 25 meters. The model was initialized at rest with a well-mixed domain where temperature and salinity are 19°C and 34, respectively (Low *et al.*, 2021). The model was forced every 10 min with depth-averaged tidal fits from adp15 (Monismith *et al.*, 2022). Hydrodynamic conditions of the domain were simulated for three months. However, the first 30 days provided dynamic adjustment of the currents. The vegetation module was activated, accounting for the drag due to the kelp forests in the simulations using the *standard* and *canopy* modules (Beudin *et al.*, 2017), and the flexibility flag (VEG_FLEX) was turned off for both scenarios. Results are presented for the second month of each simulation.

https://doi.org/10.5194/egusphere-2023-2330
Preprint. Discussion started: 30 November 2023

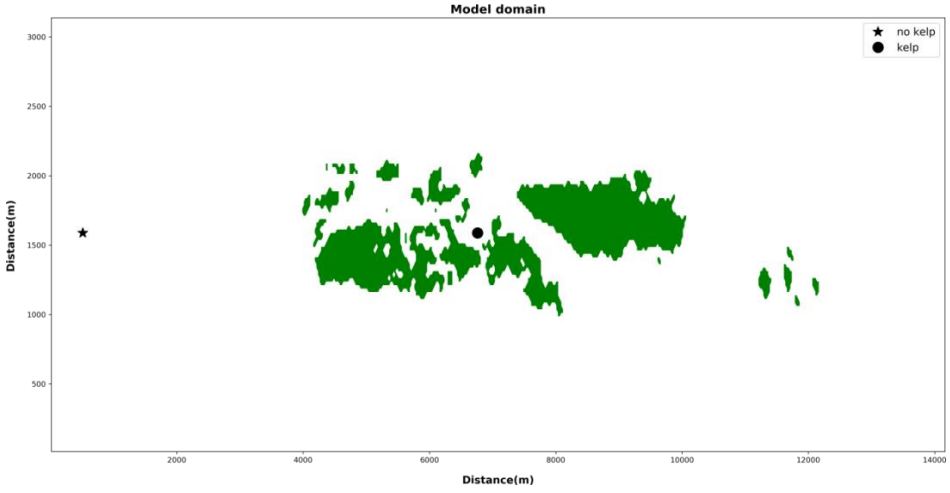

Figure 6 - Model domain. No kelp station (star) is used to validate the idealized model and kelp station (circle) is used to validate the vegetation module in *COAWST*.

3.5 Vegetation module parameters

The vegetation module is a standard component in *COAWST* (Beudin *et al.*, 2017). This module receives *u* and *v* from *ROMS* and returns both the drag force (F_d) and vertical turbulent mixing (Beudin *et al.*, 2017). The vegetation module requires 4 parameters: plant height (m), plant density (plants/m^2), plant diameter (m), and plant thickness (m) (Table 1). The other settings are number of vegetation types, Young's modulus (10^7), vegetation mass density (1000.0), additional horizontal viscosity coefficient (0.0), and drag coefficient for each individual plant (0.05-0.6).

https://doi.org/10.5194/egusphere-2023-2330
Preprint. Discussion started: 30 November 2023

Table 1 - Vegetation module initial parameters.

	Plant height(m)	Plant Density (plants/m²)	Plant diameter (m)	Plant thickness (m)
Standard	13	0.9*	0.3	0.3
Canopy			See equation 3	See equation 3

*(GAYLORD *et al.*, 2007).

3.6 Time-averaged velocity

The output velocity data were used to calculate the time-averaged velocity ($\bar{u}$). To compute $\bar{u}$, alongshore and cross-shore velocities were used to calculate velocity component in the domain, and then, integrated in time:

$$|V| = \sqrt{\bar{u}^2 + \bar{v}^2} \quad \textbf{(4)}$$

$$\bar{u} = \frac{1}{T}\int_0^T u dt \quad \textbf{(5)}$$

3.7 Model Skill

A quantitative model skill was presented by Willmott (*1981*) (eq. 6)*:*

$$WS = 1 - \frac{\sum_{i=1}^{N}(m_i - o_i)^2}{\sum_{i=1}^{N}(|m_i - \bar{o}| + |o_i - \bar{o}|)^2} \quad \textbf{(6)}$$

where *m* is the variable modeled being compared against the observed variable (*o*), the index *i* represents each depth for our case. It takes the sum of difference for each point squared and divides by sum of the absolute variability of the model and observed variable in relation to the mean of the observed variable squared. A Willmott Skill equal to 0 (WS = 0), means complete disagreement, and, *WS* = 1 means exact match between simulations and observations. This

https://doi.org/10.5194/egusphere-2023-2330
Preprint. Discussion started: 30 November 2023

verification has been applied in other model simulations (Warner *et al.*, 2005b; Liu *et al.*, 2009). Before calculating *WS*, the model was interpolated to the depths of the *adp* dataset. Time-averaged velocities for the domain with the vegetation module off and the *no kelp station* (Fig. 6) were the same, and therefore, we used *no kelp station* for the validation. The *kelp station* (Fig. 6) was used and compared against *adp*14 where kelp biomass was the highest (Fig. 4).

3.8 Bulk Drag calculations

Field estimates of kelp forest drag coefficients represent the bulk drag effect of multiple kelp plants. For example, in a 1-D linear momentum balance,

$$\frac{\partial u}{\partial t} + C_D^B \frac{U\,|U|}{h} = -g\frac{\partial \eta}{\partial x} \qquad \textbf{(7)}$$

After some manipulation:

$$C_D^B = -\frac{h(\frac{\partial u}{\partial t} + \frac{\partial \eta}{\partial x})}{U\,|U|} \qquad \textbf{(8)}$$

Applying the centered difference method for $\frac{\partial u}{\partial t}$ and $\frac{\partial \eta}{\partial x}$, yields:

$$C_D^B = \frac{-\frac{h}{2\Delta t}(u_j^{t+1} - u_j^{t-1}) - \frac{hg}{2\Delta t}(\eta_{j+1}^t - \eta_{j-1}^t}{\bar{u}\,|\bar{u}|} \qquad \textbf{(9)}$$

The bulk drag coefficient, C_D^B (eq. 9), is the net coefficient for the entire region of influence, which is not necessarily the drag force on an individual kelp plant, C_D^i. In the *COAWST* model, the drag coefficient input is for an individual plant, C_D^i. Therefore, to evaluate model input, we changed C_D^i and used the model to estimate C_D^B. Computing C_D^B does two things, 1) shows that the drag on an individual kelp plant is not the same as the bulk drag coefficient, and 2) allow us to parameterize the kelp model. In total, there were 12 simulations varying C_D^i from 0.05 to 0.6. A threshold for

https://doi.org/10.5194/egusphere-2023-2330
Preprint. Discussion started: 30 November 2023

velocities less than 0.05 m/s was imposed in order to get reasonable estimates of C_D^B during calculations.

3.9 Turbulent Kinetic Energy (TKE)

Turbulent kinetic Energy (TKE) is generally described by the intensity of the turbulent motion. The nearshore environment is believed to be an important region that dissipates TKE (Carter *et al.*, 2005). Like bottom boundary conditions in a nearshore environment, vegetation also increases TKE (Rosman *et al.*, 2010; Kalra *et al.*, 2017). For example, a laboratory study demonstrated that while kelp increased TKE in the water column when compared to no kelp, the largest turbulence occurred when the kelp had a dense surface canopy (Rosman *et al.*, 2010). TKE was calculated by *ROMS* and normalized by the total velocity. The TKE calculation was computed only for a cross-section area where kelp forest region was present.

4 RESULTS

Before starting the analysis of the kelp forest model, the model needs to adjust to a stable condition using a spin-up period to remove transient dynamics due to initial startup. For this simulation, we use sea surface elevation as the spin-up variable (Fig. 7). Because the no kelp simulation only has alongshore and cross-shore velocities as forcings, the period needed to stabilize was a little less than a month (Fig. 7-a), when kelp was added the spin-up period increased to closer to a month (Fig. 7-b). The amplitude of the sea surface height (SSH) stayed at 0.02 m and 0.001 m for no kelp and vegetation module on, respectively. There was no difference in SSH amplitude and time for the system to stabilize for both simulations *standard* and *canopy*. When the vegetation module is added, SSH amplitude decreases, representing up to 40% reduction in amplitude.

https://doi.org/10.5194/egusphere-2023-2330
Preprint. Discussion started: 30 November 2023

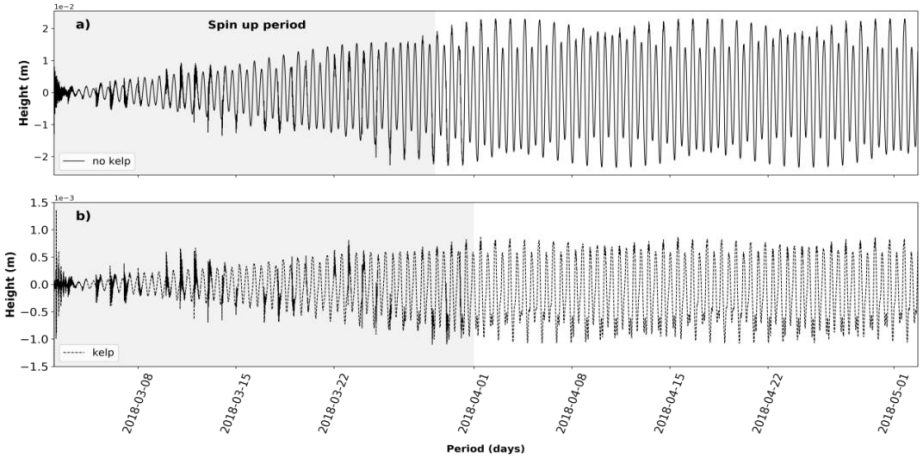

Figure 7 - Spin-up of the model domain for no kelp and inside kelp.

For the remaining analysis, the model was interpolated to the points of the *adp* dataset. The no kelp model showed good agreement with *adp15* (Fig. 8). Validation of the time-averaged currents was only possible up to 10.15 m from the bottom due to invalid values measured by the *adp15* instrument. The model overestimated the velocity over the first 4 m, underestimated it up to 9 m, and overestimated for the remainder of the data available. The absolute maximum difference was 0.008 m/s between model velocity and those observed at 6 m. The skill for the time-averaged velocity in the no kelp model run compared to *adp15* was 98.8%. A high *WS* indicates a good agreement with the variability of the observed dataset.

https://doi.org/10.5194/egusphere-2023-2330
Preprint. Discussion started: 30 November 2023

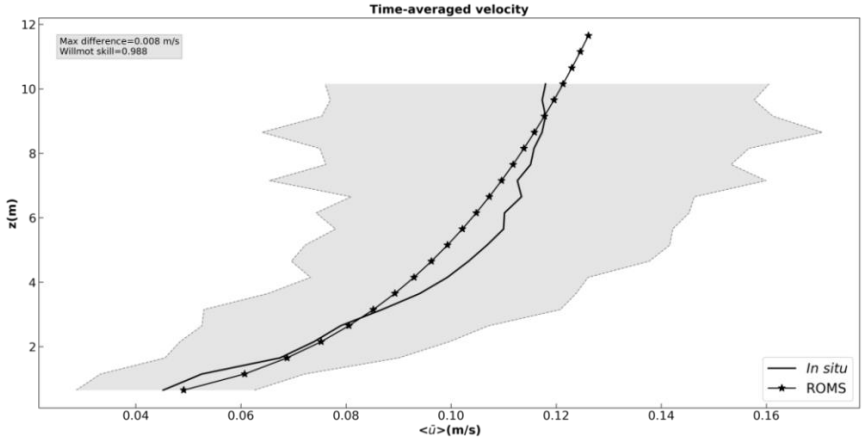

297

298 Figure 8 - Time-averaged profile comparison between *adp* data and model run without *vegetation* model.
299 The gray region shows the 95% CI and mostly represents variation in velocity due to tides. Y-axis is above
300 the bottom.

301

302 For both configurations with kelp, modeled time-averaged velocities decreased with increased
303 $C_{d,veg}$ as expected (Fig. 9). The *standard* configuration showed a slightly higher time-averaged
304 velocity than *canopy* throughout all case scenarios. This difference was more pronounced in the
305 last 4 m to the surface. $C_{d,veg}$ was a way to change the fit of the velocities in the kelp simulation.
306 Changes of 0.05 for $C_{d,veg}$ were considered a safe and fast approach to fit the best scenario while
307 not having to simulate too many scenarios. The best fit scenarios were $C_{d,veg}$ = 0.35 (Fig. 9-g) and
308 $C_{d,veg}$ = 0.4 (Fig. 9-h) for the *canopy* and *standard* models, respectively. At $C_{d,veg}$ = 0.35, the
309 *standard* model provided a better fit between 7-9 m than the *canopy* but overestimated everywhere
310 else compared to the new model. This was different for the $C_{d,veg}$ = 0.4 scenario. While the *canopy*
311 model showed a slightly better fit in the first 5 meters from the bottom, the overall best fit was
312 modeled using the *standard* approach. The higher value for the *standard* module also represents
313 the effect of not applying the effects of the kelp canopy over the entire water column.

https://doi.org/10.5194/egusphere-2023-2330
Preprint. Discussion started: 30 November 2023

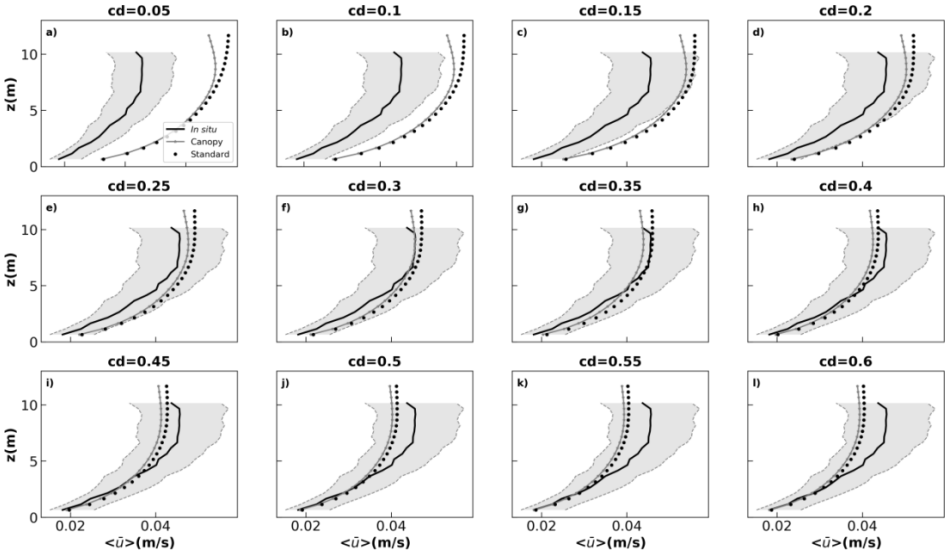

Figure 9 - Time-averaged profiles comparison between *adp* data and for standard and canopy. The gray region shows the 95% CI for the effects of the tides. Y-axis is above the bottom.

Table 2 shows *WS* calculated for the best $C_{d,veg}$ of each configuration. The water column was divided into upper and lower regions for this assessment to understand the impact of the code modification but also assess over the entire water column to check the overall fit. The division at 5 m was done because the *in-situ* data only extends to 10 m. Over the entire water column *WS* was similar. Between the two regions, both simulations had greatest skill in the first 5 m which is observable in Fig. 9g-h. The *standard* model was slightly better near the bottom. The largest difference was observed in the upper 5 m, where *canopy* model had the most skill (*WS* = 0.767). This difference is due to a slightly better fit between 5-6 m and between 8-9 m, where the velocity still feels the canopy acting on the surface velocities.

https://doi.org/10.5194/egusphere-2023-2330
Preprint. Discussion started: 30 November 2023

328 Table 2 - WS for the two best vegetation drag for both standard and canopy models.

	*top**	*down***	*total****
Standard	0.721	0.972	0.983
Canopy	0.767	0.967	0.983

329 * Calculated using values where depth is greater than 5. ** Calculated using values where depth is less or equal 5. ***Calculated for all the water
330 column.

331

332 *WS* scores separated by 0.01 m/s bins are shown in Fig. 10. Both *canopy* and *standard* simulate
333 similar along- and cross-shore velocities when compared against *in situ* datasets. *WS* values range
334 from 0.25-0.93 for alongshore velocities (Fig. 10a) and 0.19-0.47 for cross-shore velocities (Fig.
335 10b). As expected, alongshore *WS* showed better comparison than cross-shore. One possible
336 reason is that cross-shore velocities at the Punta Prieta site are also affected by internal waves and
337 tides, while surface tides dominate alongshore velocities. As a result, alongshore velocities
338 compare better with observations at higher velocities than velocities closer to zero where there can
339 be more uncertainty in both the model and measured velocities. Cross-shore velocities are best
340 simulated between 0.04 and 0.05 m/s.

341

342

https://doi.org/10.5194/egusphere-2023-2330
Preprint. Discussion started: 30 November 2023

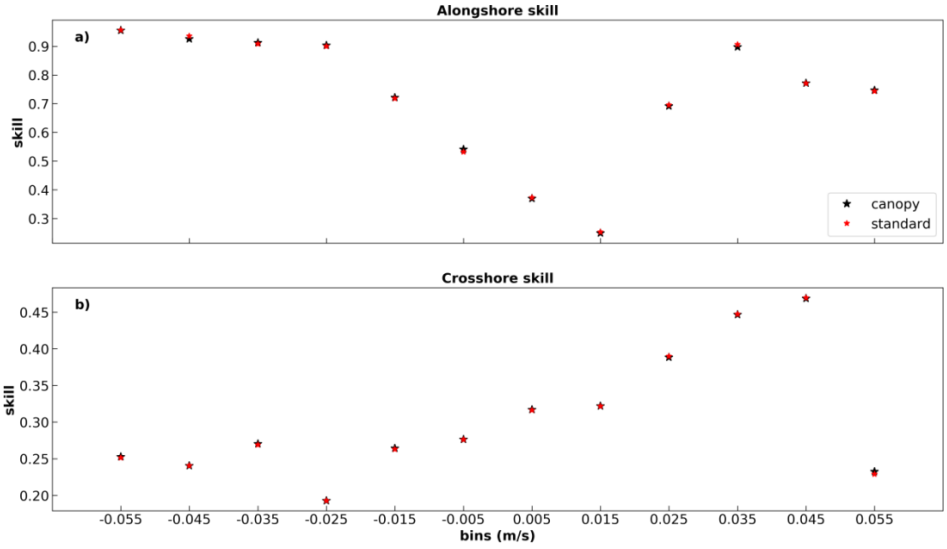

Figure 10 - WS for alongshore (a) and crosshore (b) for canopy and standard simulations split by 0.01 m/s bins.

Median bulk drag (C_D^B) increased as vegetation drag ($C_{d,veg}$) increased for both simulations (Table 3). The variability also increases as $C_{d,veg}$ becomes large. The C_D^B calculated for *canopy* is slightly larger for all $C_{d,veg}$ used. C_D^B for the best simulations were the same 0.084 and had the same variability $\pm$0.072. These values are within the values for dense kelp forests (C_D^B = 0.18) and sparse kelp forests (C_D^B=0.07) in a laboratory study (Rosman *et al.*, 2010). The values were also in agreement with Monismith *et al.*, (2022) for the *adp*15 data used for this simulation (C_D^B~ 0.04).

https://doi.org/10.5194/egusphere-2023-2330
Preprint. Discussion started: 30 November 2023

Table 3 - Median bulk drag coefficient and 95% CI calculated from **equation 7** for *standard* and *canopy*.

	Cd_{veg} = 0.05	Cd_{veg} = 0.10	Cd_{veg} = 0.15	Cd_{veg} = 0.20	Cd_{veg} = 0.25	Cd_{veg} = 0.30	Cd_{veg} = 0.35	Cd_{veg} = 0.40	Cd_{veg} = 0.45	Cd_{veg} = 0.50	Cd_{veg} = 0.55	Cd_{veg} = 0.60
***Standard*$_{cd}$**	.032± 0.016	.048± 0.028	.060± 0.037	.067± 0.045	.073± 0.052	.078± 0.059	.082± 0.065	**.084± 0.072**	.087± 0.078	.090± 0.084	.092± 0.090	.095± 0.093
***Canopy*$_{cd}$**	.036± 0.018	.052± 0.030	.064± 0.040	.071± 0.048	.077± 0.056	.081± 0.063	**.084± 0.070**	.087± 0.077	.090± 0.085	.093± 0.091	.096± 0.094	.098± 0.094

The estimates of bulk drag (C_D^B) improves as Reynolds number (Re) increases (Fig. 11). Depth-averaged velocity was binned from 0.01 m/s to 0.09 m/s with 0.01m/s intervals. C_D^B also has a Re dependency as expected. The medians for the two models are not statistically different. The C_D^B estimations are higher and less precise for smaller Re values (e.g: $10^{5.5}$ to $10^{5.8}$), and as the depth-averaged velocity increases bulk drag estimates are closer to what has been observed in the literature (Rosman *et al.*, 2010; Monismith *et al.*, 2022).

While the time-averaged profiles and bulk drag estimation are similar between both models, the difference in the mean velocity and its variability observed from the last two meters to the surface is quite different (Fig. 12). Overall, the largest differences are on the edges of the kelp forest region. The *standard* model had higher velocity and variability than *canopy* model in the last 2 m near the surface (Fig. 12a-b), resulting from the addition of kelp canopy in the latter model. *Canopy* had slightly higher velocity just below the kelp canopy especially on the edges (Fig. 12a). This decrease in time-averaged velocity at the surface and an increase at the bottom has been previously observed in laboratory for dense kelp with canopy (Rosman *et al.*, 2010; Rosman *et al.*, 2013).

https://doi.org/10.5194/egusphere-2023-2330
Preprint. Discussion started: 30 November 2023

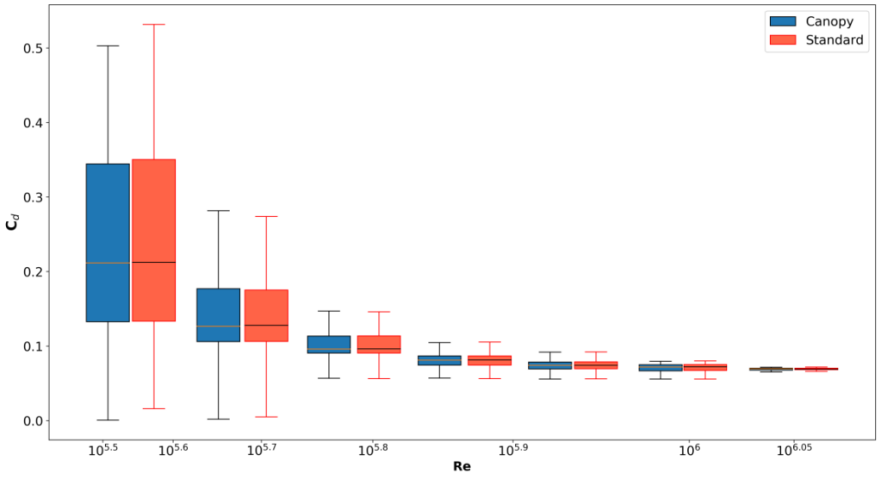

Figure 11 - Bulk drag versus Reynolds number for depth-averaged velocities at each 0.01m/s interval for both canopy and standard.

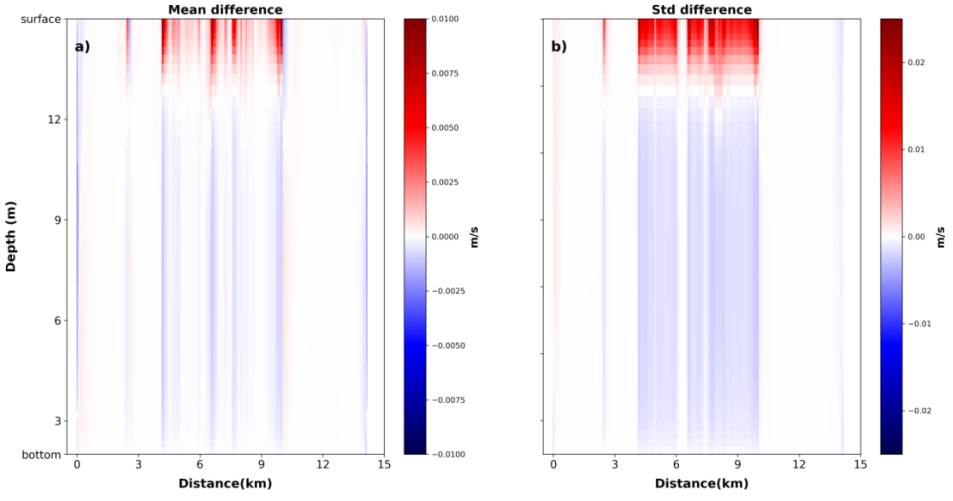

Figure 12 - Mean (a) and standard deviation (b) of velocities difference between standard and canopy. Alongshore slice at 1500m.

https://doi.org/10.5194/egusphere-2023-2330
Preprint. Discussion started: 30 November 2023

Absolute time-averaged cross-shore (Fig. 13a) and alongshore (Fig. 13b) velocities for the canopy simulation illustrate the ducting of flow around patches of kelp (Valle-Levinson et al 2022). Velocities in the kelp were disregarded, and where kelps are present in the model are shown in brown. There is an increase in mean time-averaged cross-shore speed along the outer and inner edges of the kelp forest (Fig. 13a). The highest absolute cross-shore velocities are located between kelp forests at 6.8 and 7.4 km. Flow acceleration along the edges of kelp forests has been previously observed (Jackson & Winant, 1983; Jackson, 1998; Graham, 2003). In addition, the flow channeling between kelp gaps has been described recently for the same region (Valle-Levinson *et al.*, 2022). The absolute time-averaged alongshore speeds decrease to almost zero between 1 and 1.5 km (Fig. 13b). The giant patch in front of this section is the cause of these velocities being almost null. The alongshore section shows flow channeling between 1.5 and 2 km. Flow channeling is stronger closer to the 2 km region and for depths between 8.5 m and the surface. Velocities are higher on the outer edge (approximately at 2.2 km) where there is no large patch that inhibits flows in that area. As a result, our model could also be applied to understand the effects on nutrient uptake (Gaylor *et al.*, 2007), larvae dispersal (Graham, 2003), and connectivity among beds (Gaylord *et al.*, 2006). In addition, Valle-Levinson *et al.*, (2022) hypothesized that these regions could provide localized sites of fertilization and safe spaces for various species.

https://doi.org/10.5194/egusphere-2023-2330
Preprint. Discussion started: 30 November 2023

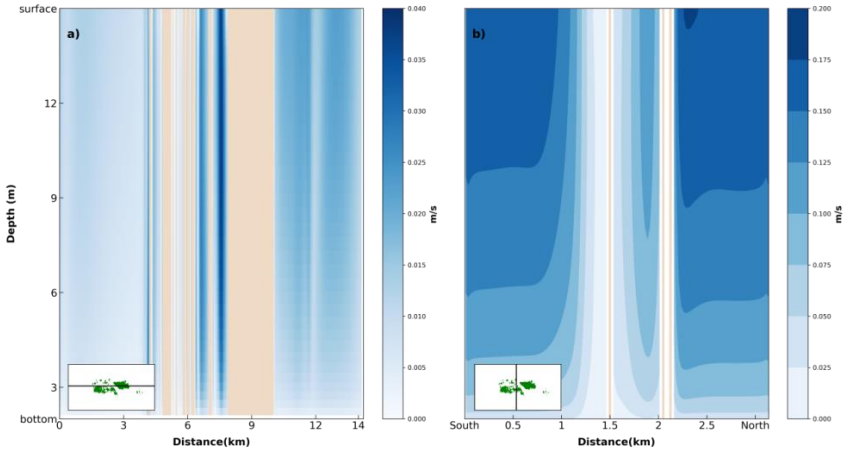

Figure 13 - Absolute time-averaged cross-shore (a) and alongshore (b) velocities for canopy module simulation. Brown region indicates where kelp forest module is present in the model.

Profiles of normalized TKE (hereafter TKE) for *standard*, *canopy*, and canopy with 50% coverage (instead of 100%) at the surface (*canopy50*) further illustrate the effects of kelp canopy on flows (Fig. 14). TKE was relatively the same from 0.5 m up to 7 m above the bottom for both the *standard* and *canopy* models. The *standard* profile is close to a linear function as expected for free surface flows. Similar mean TKE profiles were observed for no kelp and no canopy scenarios in a laboratory experiment (Rosman *et al.*, 2010). The *canopy* simulation showed a TKE peak 2-fold higher than Rosman *et al.* (2010) while *canopy50* showed values similar to this laboratory study for a dense canopy scenario. We believe this is because of the spacing at the surface in the *canopy* scenario acting as almost a solid boundary at the surface generating more friction, and therefore, more TKE. While the profiles in the Rosman *et al.* (2010) do not show the bump observed in the simulations, we observed that the peaks, for both sparse and dense with kelp fronds, are always deeper than the actual kelp fronds located at the surface which is also observed in both simulations *canopy* and *canopy50*. TKE then decreases within the canopy.

https://doi.org/10.5194/egusphere-2023-2330
Preprint. Discussion started: 30 November 2023

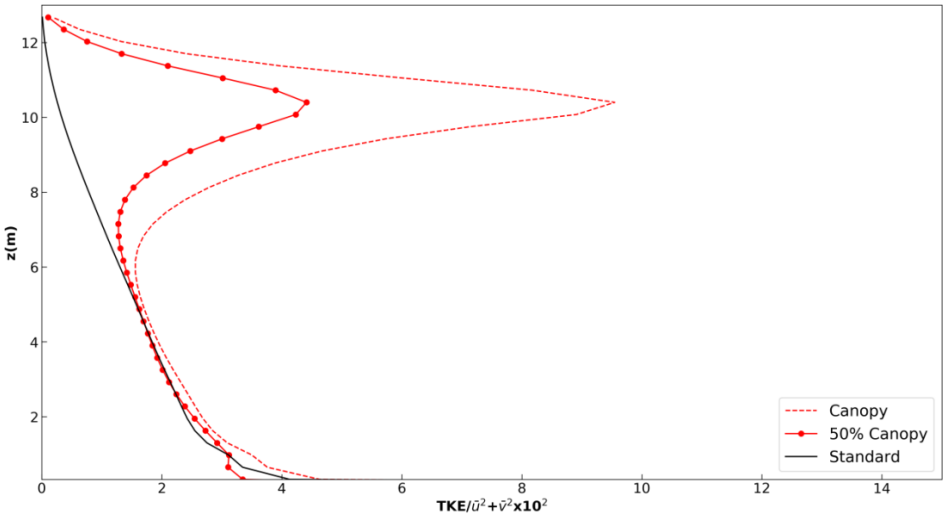

Figure 14 - Averaged normalized TKE only in the kelp forest region. Alongshore slice at 1500m.

5 DISCUSSIONS

The Coupled Ocean-Atmosphere-Wave-Sediment transport (*COAWST*) modeling system has been successfully applied to characterize wave-flow-seagrass interactions (Beudin *et al.*, 2017). The new module described in this paper, expands *COAWST* capability to simulate flow-vegetation interactions for canopied vegetation, specifically kelp forests. This module not only simulates the time-averaged tidal-driven currents in the presence of kelp forests but also the wake (turbulent kinetic energy) generated by kelp fronds as observed in laboratory experiments (Rosman *et al.*, 2010).

The influence of kelp forests on currents have been modeled previously (Wu *et al.*, 2017; Frieder *et al.*, 2022). However, these models did not explicitly account for the presence of a canopy or were run offline and thus did not provide feedback to the regional model. In this study, we implemented changes in flow and turbulence caused by kelp forests in a regional ocean model that

https://doi.org/10.5194/egusphere-2023-2330
Preprint. Discussion started: 30 November 2023

provide feedback on the flows themselves. This was possible because of the vegetation module developed by Beudin *et al.*, (2016) and our modifed approach to simulate kelp canopy. In a previous study, the effects on currents by the drag generated due to kelp forests was only implemented at the bottom of the domain (Wu *et al.*, 2017). Like this study, they also observed damping in the tidal velocity for regions where kelp beds were present. The most recent study documenting kelp forest simulation (Frieder *et al.*, 2022) not only added the changes in the flows in the water column but also simulated growth and death of kelp forests, making their model more robust than the one present here for simulating kelp effects over longer time frames. However, the shortcoming of their model was that they used an offline Large Eddy Simulation (LES) forced by model outputs, and therefore, no direct feedback in the regional ocean model. While we understand our kelp forest simulation uses a static kelp forest domain and does not show a more realistic kelp forest seasonal cycle, it does represent well the domain when kelp density is zero and when kelp density is high (0.9 plants/m^2). This module can be expanded to be used to understand the two way interaction between kelp forests, currents, and biogeochemistry, for example, and could be modified to vary parameters through time to account for growth and decay of kelp forests over seasonal and interanual cycles.

The module presented here shows good agreement for the time-averaged velocity at Punta Prieta for the 2015 period when kelp was absent (Monismith *et al.*, 2022). The differences observed mainly in the middle of the water column between our model and the *in situ* dataset could have been because the simulation was only forced with the two main tidal constituents for the domain and did not include wind and wave effects on currents (Monismith *et al.*, 2022). However, while the largest difference between model and *in situ* dataset occurs in the middle of the water column, we believe this difference could be due to two possible issues: a) model settings, for example, the

https://doi.org/10.5194/egusphere-2023-2330
Preprint. Discussion started: 30 November 2023

sigma layers being coarser in the middle of the water column, or b) not having a solid coast on the south boundary representing the island which could change the cross-shore velocities in the water column (Russell & Vennell, 2017). The upper 2 m of the water column cannot be compared due to *adp* instrument capabilities pointed out by Monismith *et al.*, (2022). This upper 2 m is strongly influenced by winds and waves that increase the velocity (see Fig. 7 in Monismith *et al.*, 2022) and for our case we did not consider these two other processes.

When kelp is present, time-averaged velocity profiles show a rapid decrease in the last meter to the surface. Neither the *standard* nor *canopy* modules captured the change in the last 2 m of the water column observed in the *in situ* datasets. When kelp is present at the Punta Prieta site, the velocities are wave-induced (Monismith *et al.*, 2022). This forcing is not imposed in the domain. Consequently, both models simulate similar patterns up to 10 meters by changing the vegetation drag by only 0.05. However, even if measurements for the last two meters are unreliable, we observe that the in situ data tends to slow down in the canopy region. The canopy region is formed due to the spread out of kelp fronds in the upper 2 m (Jackson, 1984), resulting in a dense region with larger drag than the rest of the kelp environment (Rosman *et al.*, 2010), almost like a semi-wall. Although, our *canopy* approach does not account for changes in kelp orientation with currents, it shows better results in the canopy region than the *standard* module (Fig. 12h).

The nearshore environment is believed to be a region that dissipates TKE (Carter *et al.*, 2005). Like bottom boundary conditions in a nearshore environment, vegetation increases TKE (Rosman *et al.*, 2010; Kalra *et al.*, 2017). For example, kelp forests significantly affect the various physical, chemistry, and biological processes due to the turbulence near the canopy region (Rosman *et al.*, 2010). To our knowledge, this is the first time a hydrodynamic model was able to model TKE in the water column caused by canopies.

https://doi.org/10.5194/egusphere-2023-2330
Preprint. Discussion started: 30 November 2023

The density of *M. pyrifera* plants varies significantly throughout the year (Monismith *et al.*, 2022). Reed *et al.*, (2009) found that the lowest densities were during the end of winter season while the highest were during summer. The same authors found that the spacing between canopies decrease to its minimum during fall and increase during winter. For our simulations, we found that plant density ~ 0.9 plants m^{-2} (Gaylord *et al., 2007;* Reed *et al.*, 2009) and *canopy50* produced the best scenario for summer periods, and therefore, the best fit to TKE estimates. Consequently, a study to develop a time-varying change in canopy spacing is needed to understand the impact of fronds for seasonal and yearly variability in kelp domains. Nonetheless, this new module opens opportunities to study how TKE affects nutrient availability (Rosman *et al.*, 2010), oxygen dynamics (Murie & Bourdeau, 2020), and larval transport (Pakhomov *et al.*, 2022) in kelp forest regions.

6 CONCLUSIONS

The *canopy* method presented in this paper to simulate kelp forests including the canopy is a new and relatively simple way to represent kelp forests in *COAWST*. The module modifies the plant thickness and plant diameter to decrease spacing in the last meter of the water column to mimic the effects of the kelp canopy. The revised module slightly improved fits to velocity and greatly improved fits to TKE depth profiles over the default vegetation module provided in *COAWST*. Although both the canopy and standard modules produced comparable time-averaged velocity profiles compared to the *in-situ* data, the presence of the kelp canopy resulted in a marked enhancement of turbulence near the surface. Such an improvement could considerably influence air-sea fluxes, biogeochemical processes, and the distribution of larvae within the kelp forest. This model provides improved opportunities to study the impacts of kelp forests around flows and can

https://doi.org/10.5194/egusphere-2023-2330
Preprint. Discussion started: 30 November 2023

further be used to understand larvae dispersal and biogeochemistry in a kelp environment using hydrodynamic models.

Code availability

The modified code for the **canopy** module and the codes to generate the data and figures are available at https://doi.org/10.5281/zenodo.10160564 (Fagundes and Woodson, 2023). The COAWST V3.4 source code is available from https://github.com/CSOMIO/COAWST (last access: Nov, 27th, 2023)

Author contributions

C.B.W. designed the study. M.F. conducted model runs. M.F. and C.B.W. analyzed the data. F.M, S.G.M, A.V.L. contributed significantly with constructive feedback to the science and internal discussions of the manuscript.

Disclaimer

Publisher's note: Copernicus Publications remains neutral with regard to jurisdictional claims in published maps and institutional affiliations.

Competing interests

The contact author has declared that none of the authors has any competing interests

Acknowledgments

The gratefully acknowledge support by NSF grants.

Financial support

This research has been supported by National Science Foundation (grant nos. OCE-1416837, OCE-1737090, OCE 1736830, DISES 2108566, and RISE-2108566)

References

Anderson, T. W. (1994). Role of macroalgal structure in the distribution and abundance of a temperate reef fish. *Marine ecology progress series. Oldendorf*, *113*(3), 279-290.

https://doi.org/10.5194/egusphere-2023-2330
Preprint. Discussion started: 30 November 2023

Beudin, A., Kalra, T. S., Ganju, N. K., & Warner, J. C. (2017). Development of a coupled wave-flow-vegetation interaction model. *Computers & Geosciences*, *100*, 76-86.

Boch, C. A., Micheli, F., AlNajjar, M., Monismith, S. G., Beers, J. M., Bonilla, J. C., ... & Woodson, C. B. (2018). Local oceanographic variability influences the performance of juvenile abalone under climate change. *Scientific reports*, *8*(1), 1-12.

Britton, D., Cornwall, C. E., Revill, A. T., Hurd, C. L., & Johnson, C. R. (2016). Ocean acidification reverses the positive effects of seawater pH fluctuations on growth and photosynthesis of the habitat-forming kelp, Ecklonia radiata. *Scientific reports*, *6*(1), 26036.

Campbell, N. A., & Atchley, W. R. (1981). The geometry of canonical variate analysis. *Systematic Biology*, *30*(3), 268-280.

Carter, G. S., Gregg, M. C., & Lien, R. C. (2005). Internal waves, solitary-like waves, and mixing on the Monterey Bay shelf. *Continental Shelf Research*, *25*(12-13), 1499-1520.

Cavanaugh, K. C., Reed, D. C., Bell, T. W., Castorani, M. C., & Beas-Luna, R. (2019). Spatial variability in the resistance and resilience of giant kelp in southern and Baja California to a multiyear heatwave. *Frontiers in Marine Science*, *6*, 413.

Dayton, P. K. (1985). Ecology of kelp communities. *Annual review of ecology and systematics*, *16*(1), 215-245.

Dayton, P. K., & Tegner, M. J. (1984). Catastrophic storms, El Niño, and patch stability in a southern California kelp community. *Science*, *224*(4646), 283-285.

https://doi.org/10.5194/egusphere-2023-2330
Preprint. Discussion started: 30 November 2023

Deza, A. A., & Anderson, T. W. (2010). Habitat fragmentation, patch size, and the recruitment and abundance of kelp forest fishes. *Marine Ecology Progress Series*, *416*, 229-240.

Duarte, C. M. (2017). Reviews and syntheses: Hidden forests, the role of vegetated coastal habitats in the ocean carbon budget. *Biogeosciences*, *14*(2), 301-310.

Eger, A. M., Marzinelli, E. M., Beas-Luna, R., Blain, C. O., Blamey, L. K., Byrnes, J. E., ... & Vergés, A. (2023). The value of ecosystem services in global marine kelp forests. *nature communications*, *14*(1), 1894.

Fagundes, M., & Woodson, C. B. (2023). COAWST model files. Zenodo. https://doi.org/10.5281/zenodo.10160564

Gaylord, B., Reed, D. C., Raimondi, P. T., Washburn, L., & McLean, S. R. (2002). A physically based model of macroalgal spore dispersal in the wave and current-dominated nearshore. *Ecology*, *83*(5), 1239-1251.

Gaylord, B., Rosman, J. H., Reed, D. C., Koseff, J. R., Fram, J., MacIntyre, S., ... & Mardian, B. (2007). Spatial patterns of flow and their modification within and around a giant kelp forest. *Limnology and Oceanograpy*, *52*(5), 1838-1852.

Haidvogel, D. B., Arango, H., Budgell, W. P., Cornuelle, B. D., Curchitser, E., Di Lorenzo, E., ... & Wilkin, J. (2008). Ocean forecasting in terrain-following coordinates: Formulation and skill assessment of the Regional Ocean Modeling System. *Journal of computational physics*, *227*(7), 3595-3624.

https://doi.org/10.5194/egusphere-2023-2330
Preprint. Discussion started: 30 November 2023

Kalra, T. S., Aretxabaleta, A., Seshadri, P., Ganju, N. K., & Beudin, A. (2017). Sensitivity analysis of a coupled hydrodynamic-vegetation model using the effectively subsampled quadratures method (ESQM v5. 2). *Geoscientific Model Development*, *10*(12), 4511-4523.

Ladah, L. B., Zertuche-González, J. A., & Hernández-Carmona, G. (1999). Giant kelp (Macrocystis pyrifera, Phaeophyceae) recruitment near its southern limit in Baja California after mass disappearance during ENSO 1997–1998. *Journal of Phycology*, *35*(6), 1106-1112.

Leary, P. R., Woodson, C. B., Squibb, M. E., Denny, M. W., Monismith, S. G., & Micheli, F. (2017). "Internal tide pools" prolong kelp forest hypoxic events. *Limnology and Oceanography*, *62*(6), 2864-2878.

Lentz, S. J., Kirincich, A., & Plueddemann, A. J. (2022). A note on the depth of sidelobe contamination in acoustic Doppler current profiles. *Journal of Atmospheric and Oceanic Technology*, *39*(1), 31-35.

Liu, Y., MacCready, P., Hickey, B. M., Dever, E. P., Kosro, P. M., & Banas, N. S. (2009). Evaluation of a coastal ocean circulation model for the Columbia River plume in summer 2004. *Journal of Geophysical Research: Oceans*, *114*(C2).

Low, N. H., Micheli, F., Aguilar, J. D., Arce, D. R., Boch, C. A., Bonilla, J. C., ... & Woodson, C. B. (2021). Variable coastal hypoxia exposure and drivers across the southern California Current. *Scientific reports*, *11*(1), 1-10.

Macreadie, P. I., Anton, A., Raven, J. A., Beaumont, N., Connolly, R. M., Friess, D. A., ... & Duarte, C. M. (2019). The future of Blue Carbon science. *Nature communications*, *10*(1), 3998.

https://doi.org/10.5194/egusphere-2023-2330
Preprint. Discussion started: 30 November 2023

590 Mancilla-Peraza, M., Palacios-Hernández, E., & López-Castillo, G. (1993). Hydrographic
591 Variability In Bahia Vizcaino, Baja California, Mexico. *Ciencias marinas*, *19*(3), 265-284.

592 Mcleod, E., Chmura, G. L., Bouillon, S., Salm, R., Björk, M., Duarte, C. M., ... & Silliman, B. R.
593 (2011). A blueprint for blue carbon: toward an improved understanding of the role of vegetated
594 coastal habitats in sequestering CO2. *Frontiers in Ecology and the Environment*, *9*(10), 552-560.

595 McPherson, M. L., Finger, D. J., Houskeeper, H. F., Bell, T. W., Carr, M. H., Rogers-Bennett, L.,
596 & Kudela, R. M. (2021). Large-scale shift in the structure of a kelp forest ecosystem co-occurs
597 with an epizootic and marine heatwave. *Communications biology*, *4*(1), 298.

598 Micheli, F., Saenz-Arroyo, A., Greenley, A., Vazquez, L., Espinoza Montes, J. A., Rossetto, M.,
599 & De Leo, G. A. (2012). Evidence that marine reserves enhance resilience to climatic
600 impacts. *PloS one*, *7*(7), e40832.

601 Monismith, S. G., Alnajjar, M. W., Woodson, C. B., Boch, C. A., Hernandez, A., Vazquez-Vera,
602 L., ... & Micheli, F. (2022a). Influence of kelp forest biomass on nearshore currents. *Journal of*
603 *Geophysical Research: Oceans*, *127*(7), e2021JC018333.

604 Monismith, S., Alnajjar, M., Daly, M., Valle-Levinson, A., Juarez, B., Fagundes, M., ... &
605 Woodson, C. B. (2022b). Kelp forest drag coefficients derived from tidal flow data. *Estuaries and*
606 *Coasts*, *45*(8), 2492-2503.

607 Murie, K. A., & Bourdeau, P. E. (2020). Fragmented kelp forest canopies retain their ability to
608 alter local seawater chemistry. *Scientific reports*, *10*(1), 11939.

https://doi.org/10.5194/egusphere-2023-2330
Preprint. Discussion started: 30 November 2023

609 Pakhomov, E., Kaehler, S., & McQuaid, C. (2002). Zooplankton community structure in the kelp
610 beds of the sub-Antarctic Prince Edward Archipelago: are they a refuge for larval stages?. *Polar*
611 *Biology*, *25*, 778-788.

612 Pawlowicz, R., Beardsley, B., & Lentz, S. (2002). Classical tidal harmonic analysis including error
613 estimates in MATLAB using T_TIDE. *Computers & geosciences*, *28*(8), 929-937.

614 Raffaelli, D., & Hawkins, S. J. (1996). *Intertidal ecology*. Springer Science & Business Media.

615 Reed, D., Rassweiler, A., & Arkema, K. (2009). Density derived estimates of standing crop and
616 net primary production in the giant kelp Macrocystis pyrifera. *Marine Biology*, *156*, 2077-2083.

617 Rosman, J. H., Koseff, J. R., Monismith, S. G., & Grover, J. (2007). A field investigation into the
618 effects of a kelp forest (Macrocystis pyrifera) on coastal hydrodynamics and transport. *Journal of*
619 *Geophysical Research: Oceans*, *112*(C2).

620 Rosman, J. H., Monismith, S. G., Denny, M. W., & Koseff, J. R. (2010). Currents and turbulence
621 within a kelp forest (Macrocystis pyrifera): Insights from a dynamically scaled laboratory
622 model. *Limnology and Oceanography*, *55*(3), 1145-1158.

623 Rosman, J. H., Denny, M. W., Zeller, R. B., Monismith, S. G., & Koseff, J. R. (2013). Interaction
624 of waves and currents with kelp forests (Macrocystis pyrifera): Insights from a dynamically scaled
625 laboratory model. *Limnology and Oceanography*, *58*(3), 790-802.

https://doi.org/10.5194/egusphere-2023-2330
Preprint. Discussion started: 30 November 2023

626 Russell, P., & Vennell, R. (2017). High-resolution observations of secondary circulation and
627 tidally synchronized upwelling around a coastal headland. *Journal of Geophysical Research:*
628 *Oceans*, *122*(2), 890-913.

629 Shchepetkin, A. F., & McWilliams, J. C. (2005). The regional oceanic modeling system (ROMS):
630 a split-explicit, free-surface, topography-following-coordinate oceanic model. *Ocean*
631 *modelling*, *9*(4), 347-404.

632 Schlenger, A. J., Beas-Luna, R., & Ambrose, R. F. (2021). Forecasting ocean acidification impacts
633 on kelp forest ecosystems. *PloS one*, *16*(4), e0236218.

634 Schiel, D. R., & Foster, M. S. (2015). *The biology and ecology of giant kelp forests*. Univ of
635 California Press.

636 Steneck, R. S., Graham, M. H., Bourque, B. J., Corbett, D., Erlandson, J. M., Estes, J. A., & Tegner,
637 M. J. (2002). Kelp forest ecosystems: biodiversity, stability, resilience and future. *Environmental*
638 *conservation*, *29*(4), 436-459.

639 Thomson, R. E., & Emery, W. J. (2014). *Data analysis methods in physical oceanography*.
640 Newnes.

641 Traiger, S. B., Cohn, B., Panos, D., Daly, M., Hirsh, H. K., Martone, M., ... & Nickols, K. J. (2022).
642 Limited biogeochemical modification of surface waters by kelp forest canopies: Influence of kelp
643 metabolism and site-specific hydrodynamics. *Limnology and Oceanography*, *67*(2), 392-403.

https://doi.org/10.5194/egusphere-2023-2330
Preprint. Discussion started: 30 November 2023

644 Trenberth, K. E. (1997). The definition of el nino. *Bulletin of the American Meteorological*
645 *Society*, *78*(12), 2771-2778.

646 Utter, B. D., & Denny, M. W. (1996). Wave-induced forces on the giant kelp Macrocystis pyrifera
647 (Agardh): field test of a computational model. *Journal of experimental Biology*, *199*(12), 2645-
648 2654.

649 Valle-Levinson, A., Daly, M. A., Juarez, B., Tenorio-Fernandez, L., Fagundes, M., Woodson, C.
650 B., & Monismith, S. G. (2022). Influence of kelp forests on flow around headlands. *Science of the*
651 *Total Environment*, *825*, 153952.

652 Warner, J. C., Geyer, W. R., & Lerczak, J. A. (2005). Numerical modeling of an estuary: A
653 comprehensive skill assessment. *Journal of Geophysical Research: Oceans*, *110*(C5).

654 Warner, J. C., Sherwood, C. R., Signell, R. P., Harris, C. K., & Arango, H. G. (2008). Development
655 of a three-dimensional, regional, coupled wave, current, and sediment-transport model. *Computers*
656 *& geosciences*, *34*(10), 1284-1306.

657 Walter, R. K., Woodson, C. B., Arthur, R. S., Fringer, O. B., & Monismith, S. G. (2012). Nearshore
658 internal bores and turbulent mixing in southern Monterey Bay. *Journal of Geophysical Research:*
659 *Oceans*, *117*(C7).

660 Wernberg, T., Krumhansl, K., Filbee-Dexter, K., & Pedersen, M. F. (2019). Status and trends for
661 the world's kelp forests. In *World seas: An environmental evaluation* (pp. 57-78). Academic Press

662 Willmott, C. J. (1981). On the validation of models. *Physical geography*, *2*(2), 184-194.

https://doi.org/10.5194/egusphere-2023-2330
Preprint. Discussion started: 30 November 2023

663 Woodson, C. B. (2018). The fate and impact of internal waves in nearshore ecosystems. *Annual*
664 *review of marine science*, *10*, 421-441.

665 Wu, Y., Hannah, C. G., O'Flaherty-Sproul, M., & Thupaki, P. (2017). Representing kelp forests in
666 a tidal circulation model. *Journal of Marine Systems*, *169*, 73-86.

667

668